Using Harmonic Oscillators to Determine the Spot Size of Hermite-Gaussian Laser Beams

Sidney L. Steely

Calspan Corporation / AEDC Division
MS 640, Arnold AFB, TN 37389

Abstract

This paper illustrates the similarity of the functional forms of quantum mechanical harmonic oscillators and the modes of Hermite-Gaussian laser beams. This functional similarity provides a direct correlation to investigate the spot size of large-order mode Hermite-Gaussian laser beams. The classical limits of a corresponding two-dimensional harmonic oscillator provide a definition of the spot size of Hermite-Gaussian laser beams. The classical limits of the harmonic oscillator provide integration limits for the photon probability densities of the laser-beam modes to determine the fraction of photons detected therein. Mathematica is used to integrate the probability densities for large-order beam modes and to illustrate the functional similarities. The probabilities of detecting photons within the classical limits of Hermite-Gaussian laser beams asymptotically approach unity in the limit of large-order modes, in agreement with the Correspondence Principle. The classical limits for large-order modes include all of the nodes for Hermite-Gaussian laser beams; Sturm's theorem provides a direct proof.

1. Introduction

There are many instances in science where different physical models have similar or identical functional forms. Scientists often exploit and glean ideas from other disciplines to better understand new areas of research, especially if the physical models exhibit similar functional forms. The harmonic oscillator is a powerful tool for explaining and understanding many similar disciplines of physics. Since exact solutions exist for the classical and quantum harmonic oscillator, it is a tool and simple model to understand basic principles of vibrational motion and normal modes. In addition, the harmonic oscillator is an excellent pedagogical system to help model and understand the basic properties of quantum mechanics, quantized radiation fields, quantum optics, and other disciplines of physics. Yes— the harmonic oscillator rightfully deserves its place "on a pedestal" [1].

In this paper we will exploit and use the similarity of the functional forms of quantum harmonic oscillators and Hermite-Gaussian laser beams to investigate the

spot size of laser-beam modes and the fractional energy and photons incident therein. As a result of two slightly different definitions for Hermite polynomials [2,3], some references indicate that the spot size, as delimited by the peaks of large-order Hermite-Gaussian beams, does not include most of the energy [4,5]. In view of the Correspondence Principle, the probability of finding the quantum oscillator within the classical limits asymptotically increases to unity for higher-order modes. Since the functional forms of the quantum oscillator and laser-beam mode are similar, we should expect the probability of detecting photons within the corresponding classical limits of Hermite-Gaussian laser-beam modes to similarly approach unity for higher-order modes. Mathematica [6] is used to integrate the laser-beam mode probability densities for small- and large-order modes to illustrate these principles. Sturm's theorem provides a direct proof that the classical limits also contain all of the probability density peaks. The harmonic oscillator's classical limits, therefore, serve to provide a good measure of large-order mode spot size for Hermite-Gaussian laser beams.

The classical oscillator, it's classical limits, and the classical probability density are reviewed in Section 2. Section 3 provides a discussion of the quantum oscillator, the corresponding probability densities, and the Correspondence Principle. The Hermite-Gaussian laser beam modes are reviewed in Section 4 and compared to the quantum oscillator. Section 5 provides a discussion of the Mathematica results from integrating the laser-beam mode probability densities. Sturm's theorem and its application to the peaks and zeros of the probability densities are discussed in Section 6.

2. Classical Limits and Probability Densities

Many systems oscillate by small amounts near a point of stable equilibrium. The motion of a simple system having one degree of freedom and small oscillations can be described by a simple linear harmonic oscillator. Some systems having more than one degree of freedom can also be described by a set of coupled or decoupled harmonic oscillators. Although the Lagrangian formulation is well suited for developing the theory of small oscillations [7], the Hamiltonian formulation provides a direct solution for the simple harmonic oscillator of mass m coupled to a massless spring of force constant k. The force on the mass is given by Hooke's law $F = -kx$ with the corresponding potential $V = kx^2/2$. The Hamiltonian for a harmonic oscillator can be written as the sum of a kinetic and a potential energy quadratic in the momentum p and the position x

$$\mathcal{H} = T + V = \frac{p^2}{2m} + \frac{1}{2}m\omega^2 x^2 \tag{1}$$

where $\omega^2 = k/m$ and $\omega = 2\pi\nu$ is the angular frequency of oscillation.

The equations of motion for the harmonic oscillator are obtained from Hamilton's canonical equations [7]

$$\dot{q}_i = \frac{\partial \mathcal{H}}{\partial p_i}, \quad \dot{p}_i = -\frac{\partial \mathcal{H}}{\partial q_i}. \tag{2}$$

Using Hamilton's equations (2) with the Hamiltonian given in (1), the time derivatives for the canonical variables x and p are obtained

$$\dot{x} = \frac{\partial \mathcal{H}}{\partial p} = \frac{p}{m}, \qquad \dot{p} = -\frac{\partial \mathcal{H}}{\partial x} = -m\omega^2 x. \tag{3}$$

Differentiating $\dot{x}$ with respect to time and substituting for $\dot{p}$ in (3), we obtain the standard harmonic oscillator equation

$$\ddot{x} + \omega^2 x = 0. \tag{4}$$

The solution of this harmonic oscillator equation can be written as

$$x(t) = x_0 \cos(\omega t + \phi). \tag{5}$$

The total energy E_c of the classical harmonic oscillator is a constant of the motion. Using the oscillator Hamiltonian (1) and the relationship between the momentum and velocity, $p = m\dot{x}$, the energy can be written as

$$E_c = \tfrac{1}{2}m\dot{x}^2 + \tfrac{1}{2}m\omega^2 x^2 = \tfrac{1}{2}m\omega^2 x_0^2. \tag{6}$$

For the classical harmonic oscillator, the amplitude $x_0 = \left(2E_c / k\right)^{1/2}$ is a continuous variable. The energy is, therefore, also a non-negative continuous variable; the energy can be zero or a positive value. Solving (6) for the speed of the particle

$$|\dot{x}| = \left(2E_c/m - \omega^2 x^2\right)^{1/2} = \omega\left(x_0^2 - x^2\right)^{1/2}, \tag{7}$$

we see that the particle oscillates between the classical limits. The particle obtains maximum velocity at $x = 0$ and zero velocity at the outer limits of its motion. From (5) we also see that the particle does not classically exceed $\pm x_0$.

If we measure the oscillator's position x at random, any value within the classical limits could be observed in principle. The probability for finding the particle between x and $x + dx$ is equal to the ratio of the time spent between x and $x + dx$ to the total time for one oscillation period $T = 2\pi/\omega$. Noting that the particle passes the same position twice per oscillation, we obtain the classical probability density

$$\wp_c(x)dx = \frac{2dt}{T} = \frac{2dx}{|\dot{x}|}\frac{1}{T} = \frac{2dx}{|\dot{x}|}\frac{\omega}{2\pi} = \frac{dx}{\pi\left(x_o^2 - x^2\right)^{1/2}} \qquad (8)$$
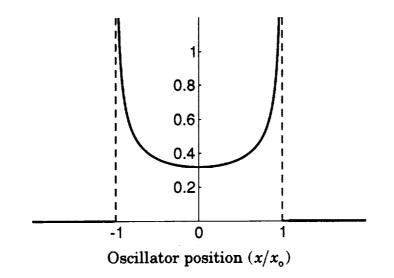
$$\wp_c(x) = \begin{cases} \dfrac{1}{\pi\left(x_o^2 - x^2\right)^{1/2}} & , \quad |x| \le x_o \\ \\ 0 & , \quad |x| > x_o . \end{cases} \qquad (9)$$

We are certain to find the classical harmonic oscillator within the classical limits $\pm x_o$; classically, the oscillator will not be observed outside the classical limits (see Fig. 1). The probability for finding the particle within the classical limits is unity and the probability for finding the particle outside the classical limits is zero, as noted by integration of (9)
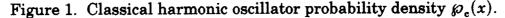
$$\int_{-x_o}^{x_o} \wp_c(x)dx = \int_{-x_o}^{x_o} \frac{dx}{\pi\left(x_o^2 - x^2\right)^{1/2}} = 1 \qquad (10a)$$

$$\int_{-\infty}^{-x_o} \wp_c(x)dx = 0 \qquad (10b)$$

$$\int_{x_o}^{\infty} \wp_c(x)dx = 0. \qquad (10c)$$

Figure 1. Classical harmonic oscillator probability density $\wp_c(x)$.

3. Quantum Mechanical Probability Densities

The quantum mechanical harmonic oscillator energy levels and eigenstates are derived from the Schrödinger equation

$$i\hbar \frac{d}{dt}|\psi\rangle = H|\psi\rangle \tag{11}$$

using the same Hamiltonian (1) where the canonical variables (x, p) are replaced with operators (X, P)

$$H = \mathcal{H}(x \to X, p \to P) = \frac{P^2}{2m} + \frac{1}{2}m\omega^2 X^2. \tag{12}$$

The eigenstates and discrete energies of the quantum harmonic oscillator are derived and discussed in many older and newer references [1,8-15]. Only the salient features are presented here in order to compare the classical and quantum oscillator probability densities with the Hermite-Gaussian laser-beam mode photon probability densities presented in Section 4.

The time-independent Schrödinger equation, as written in the X-basis representation,

$$\left(-\frac{\hbar^2}{2m}\frac{d^2}{dx^2} + \frac{1}{2}m\omega^2 x^2\right)\psi = E\psi \tag{13}$$

is solved for normalized solutions after tedious operations [1]

$$\psi_n(x) = \left(\frac{m\omega}{\pi\hbar 2^{2n}(n!)^2}\right)^{1/4} \exp\left(-\frac{m\omega x^2}{2\hbar}\right)H_n\left[\left(\frac{m\omega}{\hbar}\right)^{1/2}x\right]. \tag{14}$$

If we use $\alpha = m\omega/\hbar$ and introduce a new dimensionless variable $\xi = \sqrt{\alpha}x$, then the probability amplitude $\psi_n(\xi)$ for finding the quantum oscillator between ξ and $\xi + d\xi$ can be written in a simplified form [9,16]

$$\psi_n(\xi) = \left(\frac{1}{\pi^{1/2}2^n n!}\right)^{1/2} \exp\left(-\frac{\xi^2}{2}\right)H_n(\xi). \tag{15}$$

The Hermite polynomials $H_n(\xi)$ are nth-degree orthogonal polynomials relative to the standard weighting function $w(\xi) = e^{-\xi^2}$

$$\int_{-\infty}^{\infty} H_m(\xi) H_n(\xi) e^{-\xi^2} d\xi = \delta_{mn} \pi^{1/2} 2^n n!. \tag{16}$$

The Hermite polynomials (first four listed here)

$$H_0(\xi) = 1 \qquad\qquad H_2(\xi) = 4\xi^2 - 2$$
$$H_1(\xi) = 2\xi \qquad\qquad H_3(\xi) = 8\xi^2 - 12\xi$$

also satisfy the differential equation [3]

$$y'' + \left(2n + 1 - x^2\right)y = 0$$
$$y(x) = e^{-x^2/2} H_n(x). \tag{17}$$

In contrast to the continuous energy levels (6) of the classical harmonic oscillator, the energies of the quantum harmonic oscillator are discrete. The quantized energy values E_n correspond to the eigenstates (14) of the Schrödinger equation (13)

$$E_n = (n + 1/2)\hbar\omega. \tag{18}$$

Using (6), we see that the corresponding classical limits can be written as

$$x_0 = (\hbar/m\omega)^{1/2}(2n + 1)^{1/2}. \tag{19}$$

The smallest energy value $\hbar\omega/2$ of the quantum oscillator corresponds to the zero-state $\psi_0(x)$; the energy increases incrementally by $\Delta E_n = \hbar\omega$. The probability density $|\psi_n|^2 = \psi_n \psi_n^*$ for observing the quantum harmonic oscillator between ξ and $\xi + d\xi$ is obtained from (15)

$$|\psi_n(\xi)|^2 = \left(\frac{1}{\pi^{1/2} 2^n n!}\right) e^{-\xi^2} H_n^2(\xi). \tag{20}$$

The classical (9) and quantum (20) probability densities are plotted together in Fig. 2 for a few of the oscillator modes. As the order of the oscillator mode increases, we observe that the fraction of the area or probability to be outside of the classical limits decreases; the quantum oscillator's probability to be within the classical limits increases. We also see that the classical probability density is near the average of the quantum probability densities; this is more apparent for the large-order modes. The classical limits appear to increase with a corresponding increase in the mode order such that the outer peaks of the probability densities are always contained within the classical limits.

The classical and quantum probability densities are quite different yet similar in a number of ways. In particular, a position measurement of the quantum oscillator of energy E_n can result in any value between $-\infty$ and $+\infty$. However, when measuring the classical oscillator's position, only values between $-x_o = -\sqrt{2E_n/k}$ and $x_o = \sqrt{2E_n/k}$ will be obtained. If we consider an oscillator having a small mass of 1 gram and oscillating at 1 rad/sec with an amplitude of 1 cm, then the energy would be $m\omega^2 x_o^2/2 = 0.5$ erg. We can compare this to the energy difference between
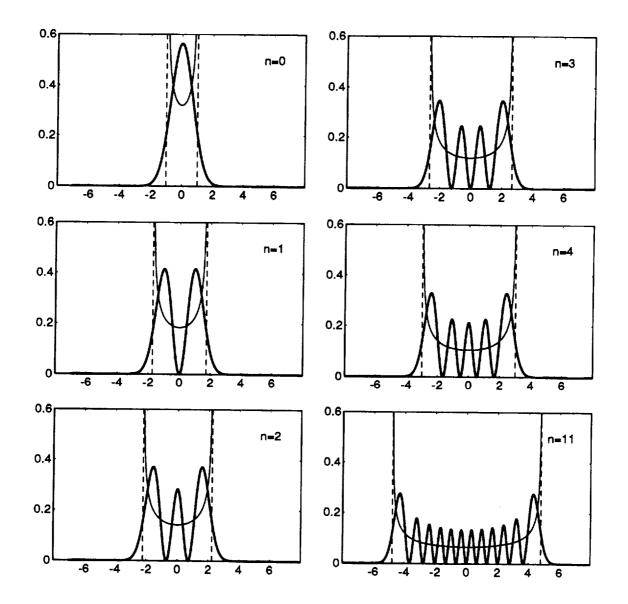

Figure 2. Quantum harmonic oscillator probability densities. (The dashed vertical lines represent the classical limits. The thin curves correspond to the classical probability densities.

the quantum oscillator levels $\Delta E = \hbar\omega \approx 10^{-27}$ erg. Experimentally it would be practically impossible to detect energy differences separated by 10^{-27} erg. Similarly, if we invert (18) to determine the mode level for this small oscillator, we see that $n = (E/\hbar\omega) - 1/2 \approx 10^{27}$. Because the mode order n is equal to the number of nodes in the quantum oscillator's probability density, it would be virtually impossible to observe 10^{27} oscillation nodes within the 2 cm interval. We would, instead, only detect or measure the average of the quantum probability density, which is just the classical result shown previously in Fig. 1. For large n, the classical and quantum results become indistinguishable as required by the Correspondence Principle [1].

In the limit of large-order modes, this special case of the Correspondence Principle illustrates how the classical picture is indeed regained. From the Correspondence Principle and the limit of large-order modes $n \to \infty$, we should expect the quantum mechanical probability densities to be functionally similar to the classical harmonic oscillator probability density. This can be derived in a number of ways [8,15]. If we examine the quantum oscillator's asymptotic functional form when the mode order increases to infinity, we find a rapid oscillatory behavior that averages out to the classical results (9) [8]

$$|\psi_n(x)|^2 \xrightarrow[\substack{\text{small } x \\ \text{and} \\ \text{large } n}]{} \begin{cases} \dfrac{2}{\pi} \dfrac{1}{\left(x_o^2 - x^2\right)^{1/2}} \cos^2\left(\dfrac{x_o x}{\alpha}\right), & \text{for even } n \\[4mm] \dfrac{2}{\pi} \dfrac{1}{\left(x_o^2 - x^2\right)^{1/2}} \sin^2\left(\dfrac{x_o x}{\alpha}\right), & \text{for odd } n. \end{cases} \qquad (21)$$

4. Hermite-Gaussian Laser Beam Modes

We now consider an Hermite-Gaussian laser beam propagating along the z direction. The laser beam considered can have different beam waists along the x and y directions. The Hermite-Gaussian laser-beam intensity or irradiance at some $+z$ direction is obtained from a scalar wave equation [17,18]. The irradiance distribution of an Hermite-Gaussian laser beam that is focused at $z = 0$ can be written as [4,19]

$$E(x,y,z) = E_o \frac{w_x(0)w_y(0)}{w_x(z)w_y(z)} \exp\left(-\frac{x^2}{w_x^2} - \frac{y^2}{w_y^2}\right) H_m^2\left(\frac{x}{w_x(z)}\right) H_n^2\left(\frac{y}{w_y(z)}\right). \qquad (22)$$

The beam waists w_x and w_y are the distances at which the lowest-order mode intensity drops to e^{-1} times the value on the optical axis (some references use an e^{-2} factor to define a beam waist). The x-axis beam waist

$$w_x(z) = w_x(0)\left(1 + \frac{z^2}{z_{o_x}^2}\right)^{1/2} \qquad (23)$$

depends on the beam parameter z_{o_x} that is a function of the wavelength λ

$$z_{o_x} = \frac{2\pi}{\lambda} w_x^2(0) \qquad (24)$$

with similar results for the y-axis waist and beam parameter.

We see that (22) is similar to the quantum harmonic oscillator density (20). The functional form of the Hermite-Gaussian laser-beam mode is similar to a two-dimensional quantum harmonic oscillator probability density. Equation (22) provides the irradiance at some position in the laser beam; with proper normalization, (22) could also be interpreted as the probability density to detect photons at some position in the laser beam. If we divide (22) by the total power in the laser beam, then the result is interpreted as a probability density to detect a photon at the corresponding position.

To determine the spot size for large-order beam modes, we consider the mean-squared value (second moment) of x and y. As an example, we look at the mean-squared value of x

$$u_x^2(z)_m = \frac{\int_{-\infty}^{\infty}\int_{-\infty}^{\infty} x^2 E(x,y,z)dxdy}{\int_{-\infty}^{\infty}\int_{-\infty}^{\infty} E(x,y,z)dxdy}. \qquad (25)$$

Substituting (22) into (25) we see that the integral is separable

$$u_x^2(z)_m = \frac{\int_{-\infty}^{\infty}\int_{-\infty}^{\infty} x^2 H_m^2\left(\frac{x}{w_x(z)}\right)H_n^2\left(\frac{y}{w_y(z)}\right)\exp\left(-\frac{x^2}{w_x^2} - \frac{y^2}{w_y^2}\right)dx\,dy}{\int_{-\infty}^{\infty}\int_{-\infty}^{\infty} H_m^2\left(\frac{x}{w_x(z)}\right)H_n^2\left(\frac{y}{w_y(z)}\right)\exp\left(-\frac{x^2}{w_x^2} - \frac{y^2}{w_y^2}\right)dx\,dy} \qquad (26)$$

and reduces to a simpler form by canceling the y-dependent factors

$$u_x^2(z)_m = \frac{\int_{-\infty}^{\infty} x^2 H_m^2\left(\frac{x}{w_x(z)}\right)\exp\left(-\frac{x^2}{w_x^2}\right)dx}{\int_{-\infty}^{\infty} H_m^2\left(\frac{x}{w_x(z)}\right)\exp\left(-\frac{x^2}{w_x^2}\right)dx} \qquad (27)$$

with a similar result obtained for the y direction. The integrals in the numerator and denominator of (27) occur frequently in quantum mechanics in relation to the harmonic oscillator problem and are readily solved using the generating function for the Hermite polynomials [13,16]

$$\int_{-\infty}^{\infty} x^2 H_m^2\left(\frac{x}{a}\right) \exp\left(-\frac{x^2}{a^2}\right) dx = 2^m \pi^{1/2} m! a^3\left(m + \frac{1}{2}\right) \tag{28}$$

$$\int_{-\infty}^{\infty} H_m^2\left(\frac{x}{a}\right) \exp\left(-\frac{x^2}{a^2}\right) dx = 2^m \pi^{1/2} m! a. \tag{29}$$

Using (28) and (29) in (27) we obtain

$$u_x^2(z)_m = w_x^2(z)(m + 1/2). \tag{30}$$

Taking the square root of twice the mean-squared value, we then obtain

$$2u_x^2(z)_m \equiv w_x^2(z)_m = w_x^2(z)(2m + 1) \tag{31}$$

$$w_x(z)_m = w_x(z)(2m + 1)^{1/2} \tag{32a}$$

$$w_y(z)_n = w_y(z)(2n + 1)^{1/2}. \tag{32b}$$

Equations (32) define the beam waists for large-order modes and depend on the order m,n of the mode. We see that the beam waists (32) have a mode order dependence that is identical to that of the classical limits of the harmonic oscillator (19). To illustrate the beam waist, two laser-beam modes are plotted in Fig. 3 along with the corresponding limits (32) that define the rectangular region and size of the laser-beam spot.
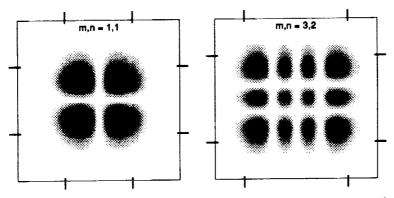

Figure 3. Photon probability density plots and classical limits for TEM$_{11}$ and TEM$_{32}$ modes. (The vertical and horizontal ticks represent the classical limits $w_x(z)_m$ and $w_y(z)_n$.)

We again see that the corresponding beam waists or "classical limits" seem to increase such that the intensity peaks are always contained therein. Since the photon probability density for an Hermite-Gaussian laser beam is identical to a two-dimensional quantum oscillator, it is expected that the probability of detecting photons within the corresponding classical limits of Hermite-Gaussian laser-beam modes will also asymptotically approach unity as the laser-beam mode order increases to infinity, that is as $m,n \rightarrow \infty$.

5. Fractional Power and Photon Probabilities

In Section 3 and 4, we saw that the classical limits seem to contain most of the probability to detect the quantum oscillator and the photons for the Hermite-Gaussian laser beams. For the large-order mode spot size to be meaningful and useful, it should contain a large portion of the power or photons of the laser beam. The probability to detect photons within the corresponding classical limits that define the spot size of the laser beam should similarly increase for large-order beams, just as in the quantum oscillator case and in agreement with the Correspondence Principle. To investigate the fraction of the power or the photon probability within the classical limits, as illustrated in Fig. 3, an integration over the classical limits is performed

$$
f_{m,n} = \frac{\underset{\text{Classical Limits}}{\iint} H_m^2(\xi)\exp\left(-\xi^2\right)H_n^2(\zeta)\exp\left(-\zeta^2\right)d\xi d\zeta}{\underset{\infty}{\iint} H_m^2(\xi)\exp\left(-\xi^2\right)H_n^2(\zeta)\exp\left(-\zeta^2\right)d\xi d\zeta} \tag{33}
$$

where $\xi = x/w_x(z)$ and $\zeta = y/w_y(z)$. Using (16) in (33) we obtain

$$
f_{m,n} = \frac{\int_{-\sqrt{2m+1}}^{\sqrt{2m+1}} H_m^2(\xi)\exp\left(-\xi^2\right)d\xi \int_{-\sqrt{2n+1}}^{\sqrt{2n+1}} H_n^2(\zeta)\exp\left(-\zeta^2\right)d\zeta}{2^{m+n}\pi m! n!}. \tag{34}
$$

The photon probabilities (34) were computed using Mathematica and are presented in Table 1 for the low-order modes. Mathematica was also used to compute the photon probabilities for higher-order modes. Figure 4 illustrates the asymptotic behavior anticipated for the higher-order Hermite-Gaussian laser beam modes. As the order of the laser-beam mode increases to infinity, we see that the probability to detect photons within the corresponding classical limits asymptotically approaches unity, as expected from the quantum oscillator problem and the Correspondence Principle. In particular, we see from Table 1 and Fig. 4 that $f_{m,n} \rightarrow 1$ as $m,n \rightarrow \infty$.

165

Table 1. Probability $f_{m,n}$ of detecting photons within the classical limits.

	m=0	1	2	3	4	5	6	7	8	9	10
n=0	0.710	0.748	0.762	0.770	0.776	0.780	0.783	0.786	0.788	0.790	0.792
1	0.748	0.789	0.803	0.812	0.818	0.822	0.826	0.828	0.831	0.833	0.835
2	0.762	0.803	0.818	0.827	0.833	0.837	0.841	0.844	0.846	0.848	0.850
3	0.770	0.812	0.827	0.836	0.842	0.846	0.850	0.853	0.855	0.857	0.859
4	0.776	0.818	0.833	0.842	0.848	0.852	0.856	0.859	0.861	0.863	0.865
5	0.780	0.822	0.837	0.846	0.852	0.857	0.861	0.863	0.866	0.868	0.870
6	0.783	0.826	0.841	0.850	0.856	0.861	0.864	0.867	0.870	0.872	0.873
7	0.786	0.828	0.844	0.853	0.859	0.863	0.867	0.870	0.872	0.875	0.876
8	0.788	0.831	0.846	0.855	0.861	0.866	0.870	0.872	0.875	0.877	0.879
9	0.790	0.833	0.848	0.857	0.863	0.868	0.872	0.875	0.877	0.879	0.881
10	0.792	0.835	0.850	0.859	0.865	0.870	0.873	0.876	0.879	0.881	0.883

6. Probability Density Nodes, Peaks, and Sturm's Theorem

It is not entirely obvious that all probability density peaks of the quantum oscillator or of the large-order Hermite-Gaussian laser beams are contained within the corresponding classical limits. The Hermite functions $y(x) = e^{-x^2/2} H_n(x)$ determine the nodes (zeros) of both the quantum oscillator densities and the Hermite-Gaussian laser-beam intensities for all modes. The nodes of orthogonal
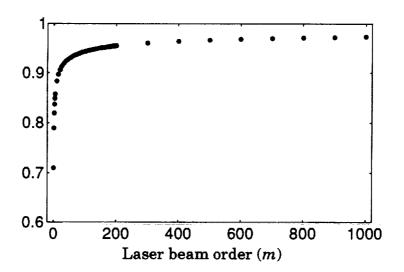

Figure 4. Plot of the probability $f_{m,m}$ of detecting photons within the classical limits of an Hermite-Gaussian laser beam.

166

polynomials are all real, distinct, and lie within the interior of the orthogonality region [20]. Figure 5 illustrates that the nodes of the Hermite functions also determine the nodes of the quantum oscillator and the Hermite-Gaussian laser beam modes.

The orthogonality region of Hermite polynomials extends from minus infinity to plus infinity as seen from the integral (16). Some method is, therefore, desired that will provide a limit to the extent of the nodes of the Hermite polynomials, the Hermite functions, and consequently the nodes of the probability densities of the quantum harmonic oscillator and of the Hermite-Gaussian laser-beam modes. Sturm's classic work on differential forms and the zeros of functions is one such method for analysis of the nodes of the Hermite functions. Sturm's theorem provides a useful method to determine the limits of the nodes in many functions, especially the classical orthogonal polynomials such as the Hermite polynomials. Direct application of Sturm's theorem [20] and (17), shows that all nodes lie within the classical limits for the quantum oscillator (19) and the Hermite-Gaussian laser beam (32).

In addition to Sturm's method, the concavity and convexity of a function is also useful. Equation (17) can be rewritten as

$$y''/y = x^2 - (2n+1) \tag{35}$$

where

$$y''/y \begin{cases} < 0, & \text{is concave for} & |x| < (2n+1)^{1/2} \\ > 0, & \text{is convex for} & |x| > (2n+1)^{1/2} \end{cases} \tag{36}$$

determines the concavity or convexity of the Hermite functions as illustrated in Fig. 6 for orders $n = 3$ and $n = 4$.
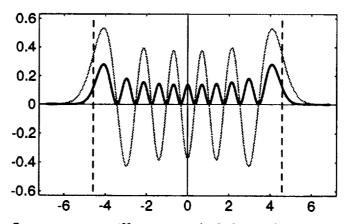

Figure 5. Quantum oscillator probability density and Hermite function of order $n = 10$. (The thick curve corresponds to the probability density. The light curve is the corresponding normalized Hermite function. Dashed lines correspond to the classical limits.)
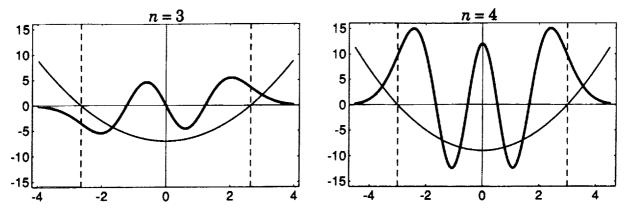
167

Figure 6. Concavity and convexity of the Hermite functions. (Thick curves denote the Hermite functions; thin curves illustrate equations (35) and (36).)

Noting the regions of concavity and convexity for the Hermite functions in (36) and Fig. 6, we see that the classical limits separate the concave and convex regions of the Hermite functions. The concave region lies between the classical limits while the convex regions lie outside of the classical limits. The classical limits always reside at inflection points of the Hermite functions and the peaks always reside within the concave region, that is, within the classical limits. We can therefore assert that the beam waists for large-order Hermite-Gaussian laser beams contain most of the laser beam power and all intensity peaks, as expected from comparison with the quantum harmonic oscillator and the Correspondence Principle.

7. Conclusions

The harmonic oscillator is indeed a useful tool to help model physical systems and, as shown in this paper, to help clarify and better understand some aspects of the probability densities of Hermite-Gaussian laser beams. In particular, the probability densities for two-dimensional quantum harmonic oscillator modes are functionally similar to the probability densities of Hermite-Gaussian laser beam modes. This functional similarity and the Correspondence Principle provide guidance to determine that the corresponding classical limits for Hermite-Gaussian laser beams define a spot size that contains a large portion of the laser beam's power. As computed with Mathematica, the portion of the Hermite-Gaussian laser-beam power or photons contained within the classical limits or beam waists asymptotically increases to unity as the laser-beam order increases to infinity. The classical limits and the corresponding laser-beam spot, as delimited by the beam waists, contain all nodes and probability density peaks of the quantum oscillator and the Hermite-Gaussian laser beams.

C-3

8. Acknowledgments

References

[1] Shankar, Ramamurti, *Principles of Quantum Mechanics*, New York, Plenum Press, 1980.

[2] Abramowitz, Milton and Irene A. Stegun, Handbook or Mathematical Functions With Formulas, Graphs, and Mathematical Tables, Washington, D. C., Government Printing Office, 1964.

[3] Magnus, Wilhelm, Fritz Oberhettinger, and Raj Pal Soni, *Formulas and Theorems for the Special Functions of Mathematical Physics*, New York, Springer-Verlag, 1966.

[4] Carter, William H., "Spot Size and Divergence for Hermite-Gaussian Beams of any Order," Applied Optics, Vol. 19, No. 7, April, pp. 1027-1029, 1980.

[5] O'Shea, Donald C., *Elements of Modern Optical Design*, New York, John Wiley & Sons, 1985.

[6] Wolfram, Stephen, *Mathematica A System for Doing Mathematics by Computer*, New York, Addison-Wesley, 1991.

[7] Goldstein, Herbert, *Classical Mechanics*, Reading, Massachusetts, Addison-Wesley, 1980.

[8] Condon, Edward and Philip M. Morse, *Quantum Mechanics*, New York, McGraw-Hill, 1929.

[9] Pauling, Linus and E. Bright Wilson, Jr., *Introduction to Quantum Mechanics*, New York, Reprinted (1965) by Dover Publications, 1935.

[10] Rojansky, Vladimir, *Introductory Quantum Mechanics*, Englewood Cliffs, New Jersey, Prentice-Hall, 1938.

[11] Messiah, A., *Quantum Mechanics*, New York, John Wiley, 1958.

[12] Leighton, Robert B., *Principles of Modern Physics*, New York, McGraw Hill, 1959.

[13] Merzbacher, E., *Quantum Mechanics*, New York, John Wiley, 1970.

[14] Sakurai, J. J., *Modern Quantum Mechanics*, Menlo Park, California, The Benjamin/Cummings Publishing Company, 1985.

[15] Gardiner, Crispin W., *Quantum Noise*, New York, Springer-Verlag, 1991.

[16] Schiff, Leonard I., *Quantum Mechanics*, New York, McGraw-Hill, 1968.

[17] Kogelnik, H. and T. Li, "Laser Beams and Resonators," Proceedings or the IEEE, Vol. 54, No. 10, pp. 1312-1329, 1966.

[18] Yariv, Amon, *Introduction to Optical Electronics*, New York, Holt Rinehart and Winston, 1971.

[19] Tompkins, Donald R. and Paul F. Rodney, "Six Parameter Gaussian Modes in Free Space," Physical Review A, Vol. 12, No. 2, August 1975.

[20] Szegö, Gabor, *Orthogonal Polynomials*, 4th Edition, Providence, Rhode Island, American Mathematical Society, 1975.

[21] Elrod, P. D., H. S. Lowry, and R. J. Johnson, "A Scene Generation Test Capability for Space Sensor Subsystems," Test Technology Symposium IV Proceedings, pp. 186-196, April 1991.

[22] Lowry, H. S., P. D. Elrod, and R. J. Johnson, "AEDC Direct Write Scene Generation Test Capability," *Beam Deflection and Scanning Technologies*, SPIE Vol. 1454, pp. 453-464, 1991.

[23] Lowry, H. S., P. D. Elrod, and T. C. Layne, "AEDC's Transportable Direct Write Scene Generation Test Capability," Accepted for presentation at the SPIE Symposium on Aerospace Sensing, Orlando, 20-24 April 1992.